



Numerical evaluation of lean premixed turbulent flame characteristics on co-axial cylinder configuration at gas turbine conditions

Siva PR Muppala, Sooraj PM Vasudevan

School of Engineering and the Environment
Faculty of Science, Engineering and Computing
Kingston University London, SW15 3DW, UK

email: s.muppala@kingston.ac.uk

Abstract

The present RANS-combustion study focuses on the flame behaviour and turbulent flame speeds at different equivalence ratios of methane/air mixtures typical of gas turbine conditions. It also highlights degree of accuracy of the Weller combustion model available in the XiFoam solver, for a set of conditions, for three equivalence ratios, for leaner mixtures (ϕ) 0.43, 0.50 and 0.56, at high pressure 5 bar and preheating temperature 673K, at bulk velocity of 40m/s. We present and discuss the flame position, turbulent flame speeds are in comparison with experimental data. This study uses two sub-models available in the Weller combustion model, to show the strong influence of equivalence ratio on above flame quantities. For lean mixture ($\phi = 0.43$), the flame shape is elliptic with increased flame brush thickness whereas for rich mixture ($\phi = 0.56$) produces a flame of conical shape of reduced flame brush thickness. We will show a good quantitative agreement between experiment and simulations. We will show that for the current geometry the turbulent strain has no much influence on laminar flame speed. Using b-Xi two-equation Weller model seems to capture the flame characteristics with more accuracy at the cost of computational time. However, with one equation model transport equation for 'b' and algebraic model for 'Xi', the results obtained are reasonably good at relatively less computational time.

Keywords: *Premixed turbulent flame, turbulent flame speed, OpenFOAM, lean mixtures, gas turbine conditions*

Introduction

Due to increased energy needs and with stress on environmental concerns, gas turbine power plants are becoming one of the promising sources of the future power needs. Gas turbine (GT) industries and researchers are coming up with innovative technologies to improve the efficiency of GT combustors and focus on reducing the emissions. These demands have led to the use of lean mixtures in gas turbines and other applications. However, one of the main drawbacks with lean mixtures is the combustion instability near flammability limits; this can be overcome by the addition of hydrogen to hydrocarbon/air mixtures. Vreman et al. [1] show that lighter fuel is more



diffusive-thermally stable and more resistant to quenching than the heavier fuel flames, resulting in a greater flame area generation. A very recent study by Benim et al. [2] showed that for turbulent swirl flows in GT combustor eddy dissipation concept in OpenFOAM yields good results, at the expense of more computational time. The burning rate per unit area correlates strongly with curvature because of preferential diffusion effects focusing fuel at positive cusps. The three-dimensional simulation clearly shows enhanced burning velocity in regions convex toward the reactants and reduced burning velocity with possible extinction in regions concave toward the reactants. To obtain these effects it was necessary to include two three-dimensional transport equations with essentially different diffusivities. Law and Kwon [3] carried out experiments to evaluate inverse effect of the potential of hydrocarbon substitution to hydrogen to improve the safety use in general and performance of IC engines. Results showed substantial reduction in the laminar burning velocities with hydrocarbon substitution, and supported the potential of propane as suppressant of both diffusive-thermal and hydrodynamic cellular instabilities in H₂/Air Flames. In a modelling approach, Muppala and Vendra [4] investigated the molecular effects of hydrocarbon substitution on turbulent H₂/Air flames using the algebraic flame surface model. This model includes the pressure and fuel type effects, and predicts a little variation in the turbulent flame speed for propane additions up to 20% by volume. However, for 50% doping turbulent flame speed reduces by 6%. Substantial reduction of turbulent flame speed with propane addition results in increase in the Lewis number of the dual-fuel mixture and proportional restriction for mobility of H₂. The concept of leading edges of the turbulent flame brush explains this decrease in flame speed. The lighter hydrocarbon substitutions tend to suppress the leading flame edges, discussed at length in a review study by Lipatnikov and Chomiak [5]. This has necessitated developing a predictive reaction model quantitatively show the strong influence of molecular transport coefficients on turbulent flame speed. This led to development of an algebraic reaction closure model previously developed [6]. Recently, RANS studies by Muppala et al. [7] studied the performance of four different reaction models for Orleans Bunsen flames and PSI flames [8].

Understanding the premixed turbulent combustion is of a high priority so that combustion can be controlled in different application scenarios. Experimental studies have given lot of insight and picture in understanding premixed turbulent combustion; Kobayashi et al.[9] conducted pioneering high-pressure experiments on a nozzle type burner with turbulence generator at high pressure to measure turbulence parameters and observe flame characteristics. These experimentalists found that the scales of turbulence generated by perforated plates at elevated pressures are smaller than at atmospheric pressure. Following features were found from flame observations, i) wrinkled structures of flame become very fine and complex, and cusps sharpen as pressure rises, ii) the flamelet breaks at many points of flame and scales of broken flamelets become small, iii) small-scale parts of the flame front convex to the reactants frequently occur and move quickly to the reactant side. Griebel and his experimental group [10] studied the effects of operating conditions and turbulence on flame front position, turbulent flame speed and flame brush thickness of lean premixed turbulent



flames at high pressures. The experiments revealed that pressure has no significant effect on the flame front position, turbulent flame speed and flame front fluctuation. For increase in fuel composition, $\phi=0.43$ to $\phi=0.56$ results in increase of turbulent flame speed by a three-fold factor. For same variation of ϕ , turbulent flame brush thickness shows increase and then decrease. In an experimental study, Yuen and Guelder [11] found that flame brush thickness tends to increase slightly with turbulence intensity whereas flame curvature decreases. Moreover, there was no significant difference in flame thickening whether flame brush thickness was measured at $b=0.5$ or $b=0.7$, and flame surface density had no dependence on turbulent intensity. This implies that the flame surface density increase by turbulence may not be a dominant mechanism for flame velocity enhancement in the flamelet combustion regime resulting in limited applicability of the flamelet approach to a much smaller regime. Nakahara et al. [12] experimentally investigated the effect of stretch on local flame properties of turbulent propagating flames of methane/propane/hydrogen mixtures with lean and rich having nearly same S_{L0} (unstrained laminar flame speed). For variation of u'/S_{L0} of 1.4 to 2, it was shown that there existed a relationship between S_F/S_{L0} and flame curvature but such trend was not seen between S_F/S_{L0} and flame stretch. This supports our finding in the numerical study by Bell et al. [13] that shows local burning rate in the methane flame is relatively insensitive to the flame curvature while the propane and hydrogen flames show strong sensitivities. For the propane flames, the burning enhances in regions of large negative curvature indicating that the flame is thermo-diffusively stable. For the thermo-diffusively unstable hydrogen flame is rigorously active in regions of positive curvature and shows pockets of local extinction when curvature is negative.

Numerical simulations help better understanding of these mechanisms and concepts involved in methane premixed lean burning. Many numerical models have been proposed and tested under various conditions several decades ago. Cant et al. [14] developed a model for reaction rate in premixed turbulent flames. *The modelling of mean reaction rate is approached by means of a library of laminar flame solutions.* They presented formulation of such a library and detailed data requirements are investigated. Importantly the flamelet properties required for the library are shown to be independent of the definition of reaction progress variable. Dinkelacker et al. [15] came up with computational model for turbulent premixed combustion where turbulent flame speed is used in an extension to a field variable to be calculated at all positions of brush in a V-shaped flame. In order to check the validation of a model, numerical results were compared with experimental data from a turbulent premixed V-shaped flame, where the conditions of the approaching turbulent flow and of the chemical processes have been varied separately. It is found to predict the flame shape and flame width sufficiently well. Flohr and Pitsch [16] suggested a turbulent flame speed closure model in the context of large-eddy simulation (LES) approach. This LES-based model was applied to a simple premixed jet flame in a backward-facing step combustor. The results predicted the forced combustor response. Benim et al. [2] shows that the EDC model in LES context has better predictive capability in gas turbine combustors. Jaravel et al. [17] used a reduced mechanism in LES to predict pollutants.

In the present study, we use the in-built Weller reaction model, tuned with subgrid-scale modelling for dynamic prediction of flame characteristics, flame speed and turbulent flame brush thickness.

We aim to numerically validate PSI experimental data by Griebel et al. [8], measured by planar LIF of the OH radical distribution along the plane through the burner axis, against flame characteristics turbulent flame speed and turbulent flame brush thickness, for three equivalence ratios at operating pressure 5 bar. Here, we use the Weller's combustion model in Xi-Foam solver[18]. For this, we invoke a two-equation model that solves transport equations for combustion regress variable 'b' and turbulent flame wrinkling parameter 'Xi'. An additional transport equation has to be solved to take into account of strain and curvature effects on laminar flame speed. To solve for Xi, algebraic and transport models are used.

2. The Weller's Premixed Combustion Model

Weller developed and implemented a closure in XiFOAM, a solver in OpenFOAM, for calculation of chemical reaction rate for turbulent premixed flames. The closure is applicable for both fully premixed and partially premixed flames in the thin reaction regimes of turbulent reacting premixed flows. It is solved with the basic governing equations mass, momentum and energy equations are solved along with turbulence KE and dissipation transport equations to take into account of turbulence. Turbulent combustion is solved in two steps, firstly, combustion is modelled using laminar flamelet assumption with single step fast chemistry approach and secondly, influence of turbulence on combustion is captured as wrinkling of the flame leading to an increase in the flame area and hence enhanced burning. The set of equations (continuity, momentum, enthalpy, regress variable and normalized turbulent flame wrinkling area) in XiFoam are,

$$\frac{\partial \rho}{\partial t} + \frac{\partial \rho U}{\partial x} = 0 \quad (\text{Eq.1})$$

$$\frac{\partial \rho U}{\partial t} + \frac{\partial \rho UV}{\partial x} = -\frac{\partial P}{\partial x} + \frac{\partial \tau_{ij}}{\partial x} \quad (\text{Eq.2})$$

$$\frac{\partial \rho h}{\partial t} + \frac{\partial \rho U h}{\partial x} = -\frac{\partial P}{\partial t} - \frac{\partial q}{\partial x} + \frac{\partial U \tau_{ij}}{\partial x} \quad (\text{Eq.3})$$

$$\frac{\partial \rho b}{\partial t} + \frac{\partial \rho U b}{\partial x} - \frac{\partial \rho}{\partial x} \left(\frac{v_t}{Sc} \frac{\partial b}{\partial x} \right) = -\rho_u S_u \left| \Xi \frac{\partial b}{\partial x} \right| \quad (\text{Eq.4})$$

$$\frac{\partial \rho \Xi}{\partial t} + \frac{\partial \rho U \Xi}{\partial x} = G \Xi - R(\Xi - 1) - (\sigma_t - \sigma_s) \Xi \quad (\text{Eq.5})$$

The flame curvature and turbulent strain effects that modify the laminar flame speed locally is modelled using sub-models. The temperature is calculated from enthalpy using Janaf coefficients through specific heat at constant pressure that is a function of



temperature. Sutherland transport model is used to calculate viscosity as a function of temperature as follows,

$$\mu = \frac{A_s \sqrt{T}}{1 + \frac{T_s}{T}} \quad (\text{Eq.6})$$

where A_s and T_s are model constants.

The model treats fuel-air mixture as one homogeneous fluid and the transport coefficients should correspond to the mixture. Hence, while solving combustion there will basically be two homogeneous fluids, one is reactants mixture and second is products mixture. The thin layer that separates reactants and products mixtures is the reaction zone or flame. A normalised fuel mass fraction value called as combustion regress variable, b is calculated in the two regions as,

$$b = \frac{Y - Y_{fuel}}{Y_{prod} - Y_{fuel}} \quad (\text{Eq.7})$$

The value of b lies between $0 < b < 1$. In the region of reactants, b takes value of 1, and b takes values 0 in the region of products. In Eq.5, Ξ is turbulence flame wrinkling which is responsible for influence of turbulence on combustion. The combustion modelling approach is based on laminar flamelet assumption that states that flame locally travels as laminar flame. The combustion happens at much smaller scales than that of turbulent flow structures. Hence, turbulence tends to wrinkle the flame surface and does not affect the chemical mechanism. The laminar flame speed stretching models and turbulent flame wrinkling models are discussed in the next sections.

2.1. Laminar flame speed models

These models take into account the straining of laminar flame speed due to flow. The straining is defined as a fractional rate of change of flame surface area given by $\frac{1}{A} \frac{dA}{dt}$.

Flame Stretch is a measure of modification of laminar flame speed by non-uniform flows, and this quantity is consists of

1. non-uniform flow, strain
2. curvature of the flame front, flame curvature effects

For the cylindrical flames, the curvature and strain effects cancel each other. Positioning of the plane of the flame front and plane of velocity gradient is a critical parameter to induce flame stretch. Velocity gradients in the direction normal to the flame front plane leads to stretching of the flame in the direction of velocity gradients [10]. In case of a steady flame with no velocity gradients in the mean flow direction and if this mean flow direction is normal to flame plane then no stretch is observed. The present geometry is an example of such a flow. Hence, no stretch is observed for



the current geometry [19]. It is however necessary to study the extent of the flame stretch effects in this in non-combustion flows. On some geometrical configurations flame stretching lowers the reaction rate and hence leads to flame extinction (Kelvin-Helmholtz instability).

S_u *Unstrained Model* assumes laminar flame speed is unaffected by strain and curvature effects. Hence S_u is fixed either based on Guelder's correlation or an experimental value. S_u *Equilibrium Model* calculates the laminar flame speed in equilibrium corresponding to local strain rate at extinction i.e. $S_u = S_{u,inf}$, where the latter quantity is calculated from strain rate corresponding to Markstein number at flame extinction. This includes a linear expression for S_u giving linear response to strain effects in the domain. The S_u *Transport Model* is applicable where strain and transport time scales are comparable with chemical time scales and thus local equilibrium assumption cannot be made. In such cases, a full transport equation has to be solved.

2.2. Turbulence flame wrinkling models

Turbulence flame wrinkling Ξ mainly takes into account of the effects of turbulence on combustion. The effect of turbulence is that it wrinkles and stretches the propagating laminar flame sheet, increasing the sheet area and, in turn, the effective flame speed. The large turbulent eddies tend to wrinkle and corrugate the flame sheet, while the small turbulent eddies, if they are smaller than the laminar flame thickness, may penetrate the flame sheet and modify the laminar flame structure. Ξ is defined as flame surface area per unit surface area resolved in the mean direction of flame propagation, denoted by, Ξ [20]. In other words, Ξ is also defined as the ratio of turbulent flame speed to laminar flame speed. The Weller's model being based on the laminar flamelet assumption follows thin reaction sheet regime that assumes flame locally propagates with laminar flame speed and wrinkled by the turbulence [18]. This effect of turbulence is captured through either an algebraic model for Ξ or a full transport equation for Ξ . One term in the *real transport equation* for Ξ includes the effects of straining the flame and another term affects the flame shape or the distribution of Ξ with respect to mean flow of the fresh mixture. Third term, from left in Eq. (5) represents the effect of differential propagation of burnt and un-burnt gases, and influence of this on the flame wrinkling. This differential propagation reduces the flame wrinkling towards region of burnt mixture and enhances the flame wrinkling on backside of the flame (towards region of fresh mixture). This term involves higher order derivatives that can create numerical difficulties. Therefore, modelling of these terms avoid the numerical instabilities and simplified as, turbulence flame wrinkling generation rate and removal rate as given below.

In the modelled transport equation for Ξ (see Eq.5), G is the rate of generation of flame wrinkling and R is the removal rate. In addition, σ_t, σ_s are local strain rates based on U , averaged effective velocity of flame surface and U_s is local instantaneous velocity of the flame surface.

On the contrary, algebraic Xi model has following expression,

$$Xi = 1 + \left\{ 1 + \left[2(0.5 - b) \right] \right\} \left(\sqrt{\frac{u'}{S_u}} \right) R_\eta \quad (\text{Eq.8})$$

where R_η Kolmogorov's Reynolds number and u' is turbulent velocity fluctuation.

This simple algebraic model is based on Guelder's correlation and DNS data for rate of generation of flame wrinkling with a linear correction function that gives a plausible profile for Xi.

Now it is the limit of the accuracy and details needed in the solution for a given problem whether to choose Xi transport or Xi algebraic model in the simulations. In the current work, we adopt both approaches for different equivalence ratios to understand the gap between the solutions obtained using Xi algebraic and Xi transport models by the Weller's flame area combustion model.

3. The Numerical Details

The RANS equations are discretised using an unstructured finite volume grid of 600,000 computational cells, after grid independency test (results not discussed). The grid is developed in ICEM taking care of fine mesh near walls (Fig.1a).

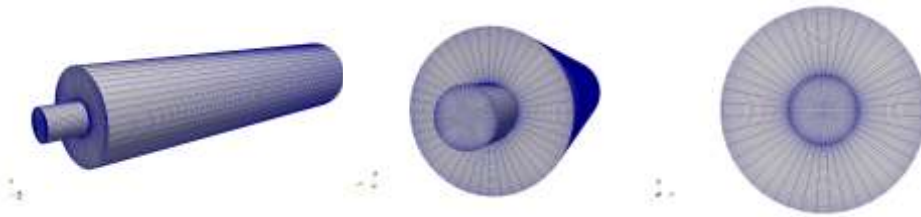


Fig.1a. The mesh of co-axial cylinder (for from L to R: full view, angled view and front view), for dimensions given in Fig. 1b.

The first order Euler schemes are used in time, second order linear differencing schemes are used for velocity. Second order Gaussian integration is used for gradient terms and Laplacian terms are solved using second order Gaussian linear interpolation schemes with non-orthogonal correction. Pressure-Velocity decoupling is done using PIMPLE algorithm, in which pressure-velocity are decoupled through Poisson equation which is derived from discretised equations of the continuity and momentum. PIMPLE algorithm is a blend of SIMPLE and PISO algorithms. Acoustic waves are eliminated from the model by making low Mach number assumption. The set of governing equations are solved one after the other over the explicit coupling terms (in Poisson equation) to obtain convergence. This segregated solution requires numerical stability criteria (CFL). The courant number $C=0.2$ is maintained for all the simulations [20].

The boundary conditions are, at inlet Dirichlet boundary conditions apply for all the quantities except for pressure that is applied with zero Neumann boundary condition. At the outlet, all the quantities are applied zero Neumann boundary

condition and Dirichlet boundary condition for pressure. The turbulent kinetic energy, k and turbulent dissipation rate (Eq.9), ϵ are given by

$$k = \frac{1}{2} (U_x'^2 + U_y'^2 + U_z'^2) \quad (\text{Eq.9})$$
$$\epsilon = \frac{C_\mu^{0.75} k^{1.5}}{l}$$

Here, the turbulent length scale l is 3 mm and turbulent velocity fluctuation is taken as $u' = 5\%$ of U . The value unstrained laminar flame speed as input comes from experiments.

4. Problem Description and case set up

The domain is designed and developed based on the experimental set up, with studies conducted at Paul Scherrer Institute (PSI), Switzerland [10]. Experimentalists studied flame characteristics at different equivalence ratios. The PIV measurements of flow field and planar LIF of OH radical distribution were used. In our numerical studies, we have taken studied for reacting flows for premixed methane/air mixtures at (673 K, 5bar) at bulk flow velocity of 40 m/s with equivalence ratio varied from $\phi = 0.43$ to $\phi = 0.56$. The computational domain is shown below:

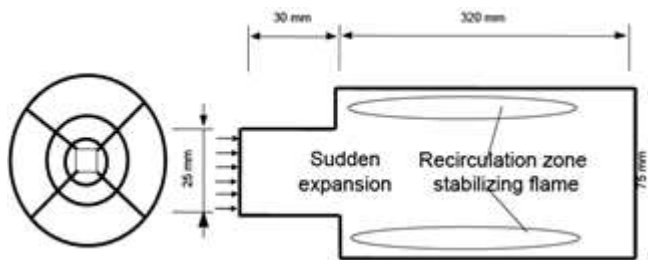


Figure 1b: The problem domain, a co-axial cylinder with turbulence grid in the 25mm-dia cylinder.

The domain consists of co-axial–25 mm dia x 30 mm length plus 75 mm dia x 320 mm length–cylindrical chamber, as shown in Fig. 1b. The short pre-inlet pipe ensures evolution of homogeneous turbulent flow entering the combustion chamber.

5. Role of Ultra-Lean Mixtures in Gas turbines

The quality of combustible mixture decides the final temperature and hence the heat release in the system. Richer the mixture more the combustion temperature due to higher fuel concentration with higher reaction rates. The high combustion temperatures in the combusting systems means higher NO_x emissions, high heat energy loss to combustion chamber walls and hence low energy efficiency. These are the mainly targeted parameters to be improved while designing a combusting device. The two essential factors resulting in NO_x emissions are first, high combustion temperature of the order 1600 K and second, high residence time of the products in the combustion chamber.

In gas turbine combustion devices used for power generation, low-temperature operation is a necessity, to achieve low NO_x emissions, to avoid overheating of the material and to enhance thermal efficiency. Lean mixture combustion is characterised by low combustion temperatures hence helps in drastic reduction of emissions. In the same direction, attempts are being made to design ultra-low emission devices taking global effects of environment into consideration.

Keeping all these factors in mind it has been usual practice to run gas turbines with leaner mixtures for industrial applications. Sometimes the mixtures are made so leaner that, there will be fear of mixtures going to threshold of lean flammability limit. Therefore, it is necessary to study the combustion behaviour of such lean mixtures and standardize the safe operating conditions for lean mixture operating combustion devices.

6. Results and Discussion

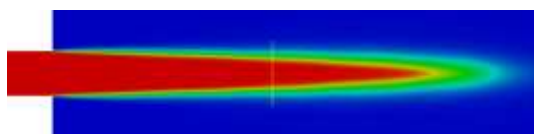
The simulations are carried out for three equivalence ratios $\phi=0.43$, $\phi=0.50$ and $\phi=0.56$. For each equivalence ratio, six different simulations are carried out in combination with different S_u and ξ_i models. This study with detailed S_u and ξ_i models is carried out to understand to what reasonable accuracy can be obtained using algebraic model or transport model for ξ_i and also study the effects flame curvature and turbulent strain on laminar flame speed for current geometry configuration.

The numerical results obtained with different S_u and ξ_i models are discussed in the next sections. We then choose the best suitable model that is able to predict the reasonable results will be taken forward for the analysis of combustion behaviour at different equivalence ratios.

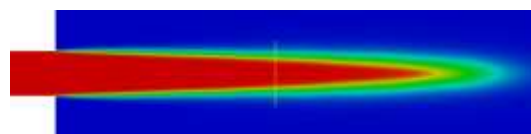
6.1. Different S_u Models, effect of Flame stretch

The prediction of different S_u models that mainly take into account of flame stretch and flame curvature, in ξ_i -Foam are:

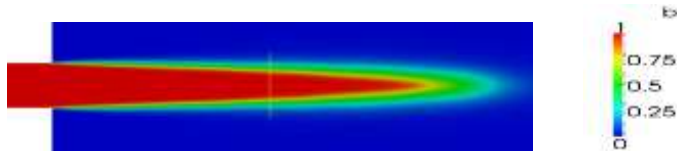
1. S_u Unstrained – laminar flame speed is un-affected by strain and curvature
2. S_u Equilibrium – laminar flame speed is in equilibrium with local strain
3. S_u Transport – a full transport equation is solved for introducing the strain effects on laminar flame speed.



S_u – Unstrained model



S_u - Equilibrium model



Su - transport model

Fig. 2. 'b' regress variable contours for Xi transport model in combination with three Su models, for the equivalence ratio $\phi=0.43$. Colour convention blue ($b=0$) is burnt or combustion gas and red ($b=1$) is un-burnt or inlet premixed gas with $0 < b < 1$.

From the figure 2 it can be observed that there is no much difference between the results obtained with S_u -Unstrained model and other S_u models. It implies that there is no effect of flame curvature or strain on the laminar flame speed for the current geometry. To make sure that this is correct, the same study is carried out with equivalence ratio $\phi=0.5$ and 0.56 . The contours obtained for equivalence ratio $\phi=0.5$ are as shown below,

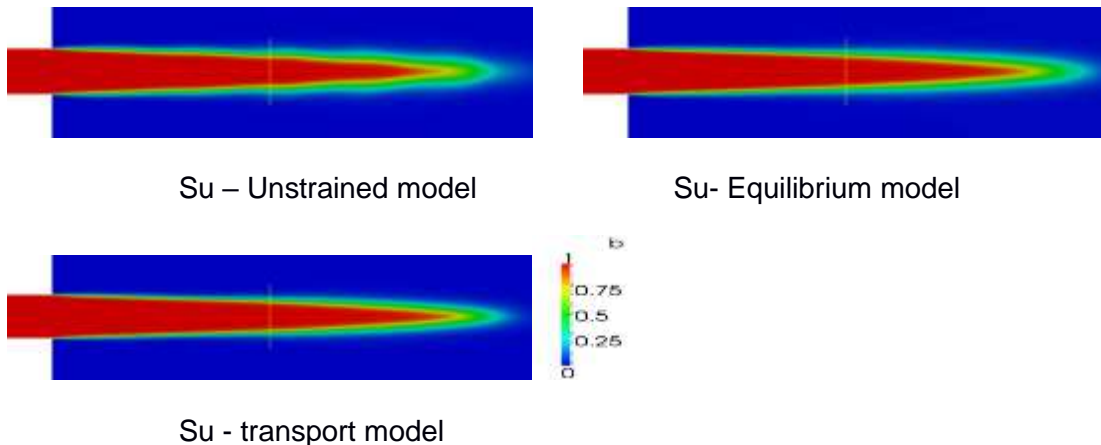


Fig.3 'b' regress variable contours for Xi transport model in combination with three S_u models, for the equivalence ratio $\phi=0.5$. Colour convention blue ($b=0$) is burnt or combustion gas and red ($b=1$) is un-burnt or inlet premixed gas with $0 < b < 1$.

From the fig 2 and 3, it is understood that there are no stretch effects in case of the current geometry. Similar results are obtained for $\phi=0.56$ and for all the S_u models in combination with Xi algebraic model for three ϕ s, hence not included. As discussed in the previous section, a possible reason for observing zero stretch may be for a cylindrical geometry the curvature and strain effects cancel each other. And another possibility for having zero stretch could be the flow domain is having uniform area duct, where at steady state no velocity gradients are present in the direction normal to the reaction sheet (i.e. in the direction of mean flow or along axis of the combustion chamber). Velocity gradients in the mean flow direction are critical in stretching the flame. Even though there is an expansion step from 25mm to 75mm in the domain near the inlet, but flame is not stabilised near this region but is stabilised far downstream from this expansion step hence no effect of this step on the flame is observed.

Note: - Since there is no effect of flame stretch on the results, from now on Su unstrained model results are not included for further discussions.

6.2. Results with Xi algebraic and Xi transport Models

The simulations are carried with Xi algebraic and Xi transport models for $\phi=0.43$, $\phi=0.50$ and $\phi=0.56$. Figure 4 shows the contours for combustion regress variable 'b'

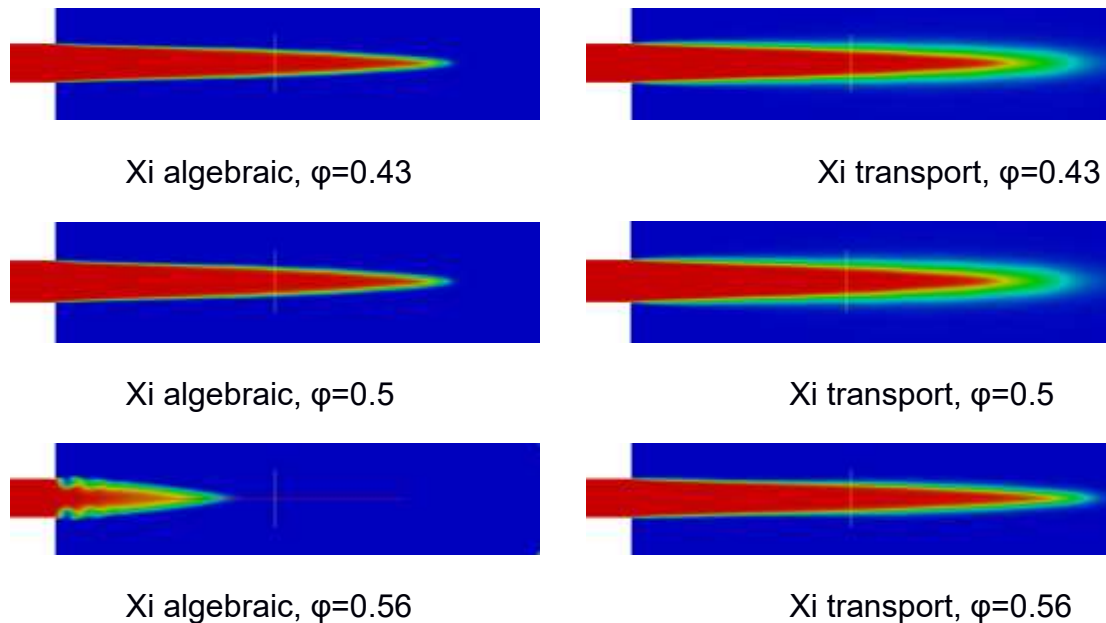


Fig.4 'b' regress variable contours for three equivalence ratios $\phi=0.43$, $\phi=0.56$ and $\phi=0.56$ in combination with Xi algebraic and Xi transport models. *Colour convention* blue ($b=0$) is burnt or combustion gas and red ($b=1$) is un-burnt or inlet premixed gas with $0 < b < 1$.

Figure 4 shows the flame contours obtained for different equivalence ratios in combination with Xi models. For equivalence ratio 0.43 and 0.5 mixtures it can be seen that the flame length predicted is nearly same for both Xi models whereas there is a discrepancy in predicting the flame brush thickness by the two Xi models. The Xi transport model predicts flame brush thickness quite reasonably well whereas Xi algebraic model does not predict the flame brush thickness. For equivalence ratio 0.56, we find a completely different behaviour, where Xi algebraic model predicts a short flame with flame brush thickness better than the flame brush thickness of cases with equivalence ratios 0.43 and 0.50 is observed. Whereas Xi transport model predicted longer flame with sharp conical end with reasonable flame brush thickness. This conical end flame is evident for rich fuel mixture leading to such shaped flame.

Xi transport model is capable of showing flame shape change behaviour with equivalence ratio with reasonable flame brush thickness, but it is not clear why this model is not showing the flame length variation with change in equivalence ratio. The terms in the Xi transport model, turbulence flame wrinkling generation behind the flame and removal at front of the flame due to differential propagation of burnt and un-burnt

gases leads to prediction of flame brush thickness and flame shape phenomenon. Whereas in Xi algebraic model no such effects have been included and is modelled just to give flame profile [4].

Another observation made is that, for equivalence ratio $\phi=0.56$, the Xi algebraic model becomes unstable with some kind of hot spots near the outlet boundary and takes more time to converge as compared to any other simulations. The flame profile obtained is more corrugated and short. On the other hand for $\phi=0.56$ with Xi transport model no such instability is observed and simulations converged smoothly.

Such an instability or convergence problem with Xi algebraic model was not observed for equivalence ratios $\phi=0.43$ and $\phi=0.5$. This could be due to the fact that as the mixture gets richer the fuel concentration increases leading to more combustion and higher heat release, which in-turn enhance reaction rate and final temperature. The algebraic model may find it difficult to resolve these high gradients.

Note: - Since Xi algebraic model is not consistent in giving results at different equivalence ratios, particularly in predicting flame brush thickness, Xi transport model has been chosen to discuss further results.

6.3. Results at different equivalence ratios

The results for the three equivalence ratios $\phi=0.43$, 0.5 and 0.56 are presented in this section. The comparison studies highlight combustion behaviour at different equivalence ratios and are compared with experiments. Equivalence ratio of a mixture decides the quality of premixed gas entering combustion chamber. Higher the equivalence ratio richer is the mixture with fuel and higher the chemical energy released. The various parameters studied and compared with experiments have been discussed in subsequent sections.

6.3.1. Flame characteristics with equivalence ratio $\phi=0.43$

Flame characteristics of methane/air mixtures with equivalence ratio $\phi=0.43$ are discussed in this section. Following contours give the various combustion parameters obtained with Su- Unstrained and Xi – Transport models.

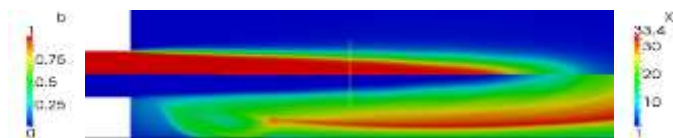


Fig.5. The upper half of figure shows the combustion regress variable b contour and lower half contour is of turbulence flame wrinkling

Figure 5 shows a smooth flame profile with an elliptical shape. The flame shape is bulged because of the un-burnt mixture being very lean i.e. low fuel concentration and thus low chemical reaction rate. Due to this fact the flame is stabilised far downstream of the domain. The peak temperature attained is 1651K and this value is been in good agreement with theoretical value. The peak temperature also corresponds to adiabatic flame temperature in this configuration as all the walls of the domain have been taken

as adiabatic. The unstrained laminar Flame speed value is taken from experiments $S_u = 0.118$. Figure 6 shows corresponding mean velocity and turbulent kinetic energy, for $\phi=0.43$.

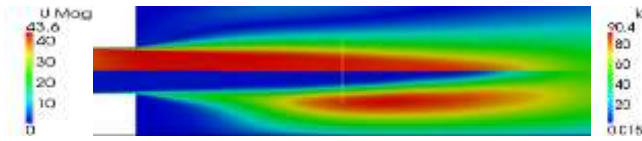


Fig.6. The upper half of figure shows the bulk velocity U contour and lower half contour is of turbulence kinetic energy k

Table 1 gives the experimental parameters obtained in comparison with numerical simulations.

Table.1. For $\phi=0.43$: Comparison of numerical flame quantities with experiments

Flame quantity	Experiment	Numerical
Flame brush thickness	31 mm	41 mm
Turbulent Flame Speed, S_T	0.59 m/s	0.47 m/s

Table 1 shows a good congruity between experiment and simulations, for both flame brush thickness and turbulent flame speed.

6.3.2. Flame characteristics with equivalence ratio $\phi=0.5$

Flame characteristics of methane/air mixtures with equivalence ratio $\phi=0.5$ are discussed in this section. Following contours give the various combustion parameters obtained with S_u - Unstrained and ξ – transport models.

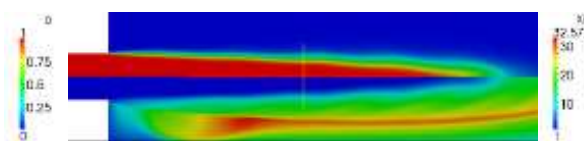


Fig.7. The upper half of figure shows the combustion regress variable b contour and lower half contour is of turbulence flame wrinkling

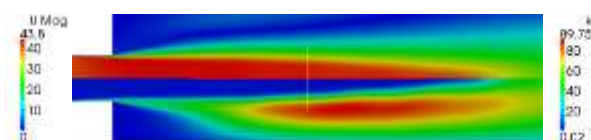


Fig.8. The upper half of figure shows the bulk velocity U contour and lower half contour is turbulence kinetic energy k

Table 2 shows the results are in close proximity between simulation and experiment with former giving a lower value. It is interesting to notice that the model over predicts turbulent flame speed.

Table.2. Comparison of numerical flame quantities with experiments, for $\phi=0.5$

Flame quantity	Experiment	Numerical
Flame brush thickness	45 mm	33 mm
Turbulent Flame Speed, S_T	1.21 m/s	1.20 m/s

For this case, the experimental value of $S_u = 0.237$ is taken. Table 2 shows S_T is in closer proximity to that of experiment, both shown increase in S_T with fuel composition. With increase in ϕ the model predicts slightly shorter flame brush thickness compared to that for $\phi=0.43$. This finding does not align well with the experiments that show increase and then decrease variation. The model exactly quantifies experiment. As can be observed in figures 7 and 8, the turbulent kinetic energy values are nearly equal for $\phi=0.43$ and $\phi=0.5$.

6.3.3. Flame characteristics with equivalence ratio $\phi=0.56$

Fig. 9 show flame characteristics of methane/air mixtures with equivalence ratio $\phi=0.56$ are discussed in this section. Following contours give the various combustion parameters obtained with Su- Unstrained and Xi – Transport models. Fig. 10 shows the mean flow velocity and turbulent kinetic energy for $\phi=0.56$.

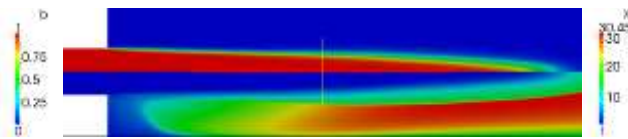


Fig.9. The upper half of figure shows the combustion regress variable b contour and lower half contour is of turbulence flame wrinkling

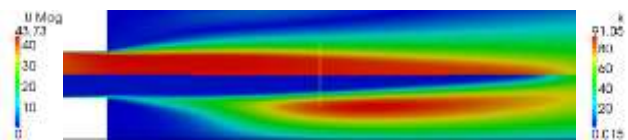


Fig.10. The upper half of figure shows the bulk velocity U contour and lower half contour is turbulence kinetic energy k

Table 3. The experimental values for $\phi=0.56$ in comparison with numerical simulations results.

Flame quantity	Experiment	Numerical
Flame brush thickness	35 mm	26 mm
Turbulent Flame Speed, S_T	1.88 m/s	3.62 m/s

Table 3 yields more satisfactory closeness experiments for S_T . This simulation case with unstrained laminar flame speed value is taken from experiment, $S_u = 0.345$. The flame brush thickness from experiments is not showing either increasing or decreasing



trend with equivalence ratio, the value has increased from 31 mm at $\phi=0.43$ to 45 mm at $\phi=0.5$ whereas decreased from 45 mm at $\phi=0.5$ to 35 mm at $\phi=0.56$. However, simulations showed decreasing trend for flame brush thickness value continuously. Similarly, S_T continues to increase from $\phi=0.43$ to $\phi=0.56$ whereas actually flame length should decrease from $\phi=0.43$ to $\phi=0.56$. The simulated S_T nearly double the measured value, 1.88 m/s. For this mixture, the turbulent kinetic energy peak marginally shifts in the flow direction by half the inlet diameter 25 mm i.e. the location is eleven times from the expansion inlet whilst this peak is at ten times the inlet diameter for the other two leaner mixtures.

Conclusions

The RANS numerical combustion study was carried out on a PSI high-pressure test rig for methane/air lean mixtures for equivalence ratios $\phi=0.43$ to $\phi=0.56$, bulk velocity of 40 m/s and high pressure 5 bar. Turbulent premixed flame behaviour and its characteristics are studied using the Weller's flame area model. The model predicted flame brush thickness, decreasing trend with ϕ . The shape of the flame changed from parabolic to conical with lower brush thickness and higher turbulent flame speed for richer mixtures and in very good quantitative agreement for $\phi=0.43$ to 0.50. However, the Weller's model is sensitive to the flame brush thickness that decreases with increase in equivalence ratio. The simulations showed that for the present geometry, turbulent strain and flame curvature have no influence on laminar flame speed. The model partly over predicts for $\phi=0.56$, that may require model tuning. Overall, the simulations offer very good consistency with experiments for leaner mixtures and are a good choice for ultra-lean mixtures.

References

1. Vreman, A.W., van Oijen, J.A., de Goey, L.P.H., and Bastiaans, R.J.M. (2009) *Direct Numerical Simulation of hydrogen addition in turbulent premixed Bunsen Flames using flamelet-generated manifold reduction*. Int. J. Hydrogen Energy, 2009. 34: p. 2778-2788.
2. Benim, A.C.I., S. Meier, W. Joos, F. Wiedermann, A. (2017) *Numerical investigation of turbulent swirling flames with validation in a gas turbine model combustor*. Applied Thermal Engineering, 110: p. 202-212.
3. Law, C.K. and Kwon, O.C. (2004) *Effects of hydrocarbon substitution on atmospheric H₂/Air flame propagation*. Int. J. Hydrogen Energy. 29: p. 867-879.
4. Muppala, S.P.R., and Vendra C Madhav Rao (2018). *Numerical Implementation and validation of turbulent premixed combustion model for lean mixtures in Inter. Conf. on Combustion Physics and Chemistry (ComPhysChem'18)*. Samara, Russia: MATEC Web of Conferences, edpsciences.org.
5. Lipatnikov, A.N. and Chomiak, J. (2005) *Molecular transport effects on turbulent flame propagation and structure*. Progress in Energy and Combustion Science. 31: p. 1-71.



6. Muppala S.P.R, A., N.K., Dinkelacker, F., Leipertz, A. (2005) *Development of an algebraic reaction rate closure for the numerical calculation of turbulent premixed methane, ethylene, and propane/air flames for pressure up to 1.0 MPa*. Combust. and Flame. 140: p. 257-266.
7. Muppala, S.P.R., Vendra, C. Madhav Rao., and Aluri, Naresh K. (2019) *Modelling and numerical simulation of dual fuel lean flames using local burning velocity and critical chemical timescale*. SAE International Journal of Engines. 12: p. 373-385.
8. Griebel, P., Boschek, E., and Jansohn, P. (2007) *Lean Blowout Limits and NOx Emissions of Turbulent Lean Premixed Hydrogen-Enriched Methane/Air Flames at High Pressure*. J. Eng. Gas Turbines Power. 129(2): p. 404-410.
9. Kobayashi, H., Nakashima, T., Tamura, T., Maruta, K., Niioka, T. , *Turbulence measurements and Observations of Turbulent Flames at elevated pressures up to 3.0MPa*. Combust. and Flame, 1997. 108: p. 104-117.
10. Griebel, P., Bombach, R., Inauen, A., Schären R. *Flame characteristics and turbulent flame speeds of turbulent, high-pressure, lean premixed methane/air flame*. in ASME Turbo Expo. 2005.
11. Yuen, F.T.C. and Guelder, O.L. *Dynamics of Lean-Premixed Turbulent Combustion at High Turbulent Intensities*. Combustion Science and Tech, 2010. 182: p. 544-558.
12. Nakahara, M., Kido, H., Shirasuna, T., Hirata, K, *Effect of stretch on local burning velocity of premixed turbulent flames*. Journal of Thermal Science and Technology, 2007. 2(2): p. 268-280.
13. Bell, J., Cheng R.K., Daylan, M.S., Shepherd, G. *Numerical Simulation of Lewis Number effects on lean premixed turbulent flames*. Proceedings of The Combustion Institute, 2007. 31(1): p. 1309-1317.
14. Cant, R.S., Rogg, B., Bray, K.B.C. *Short Communication on Laminar Flamelet modelling of the mean reaction rate in a premixed turbulent flames*. Combustion, Science and Tech, 1990. 69: p. 53-61.
15. Dinkelacker, F. and Hölzer , S. *Investigation of a Turbulent Flame Speed Closure Approach for premixed flame calculations*. Combustion, Science and Tech., 2000. 158: p. 321-340.
16. Flohr, P. and Pistch., H. *A turbulent flame speed closure model for LES of industrial burner flows*. in Centre for Turbulent research, Proceedings of the summer program. 2000.
17. Jaravel, T.R., E. Cuenot, B. Bulat, G., *Large Eddy Simulation of an industrial gas turbine combustor using reduced chemistry with accurate pollutant prediction*. . Proceedings of the Combustion Institute, 2017. 36(3): p. 3817-3825.
18. Weller, H.G., Tabor, G., Gosman, A.D., and Fureby, C., *Application of a Flame-Wrinkling LES Combustion Model to a Turbulent Mixing Layer*. . Proceedings of the Combustion Institute., 1998. 27: p. 899-907.
19. Aluri, N.K., Muppala SPR, and Dinkelacker F., *Large Eddy Simulation of Lean Premixed Turbulent Flames of Three Different Combustion Configurations using a novel Reaction closure*. Flow Turbulence Combust, 2008. 80: p. 207-224.
20. www.openfoam.org.